Geophysical Journal International

Geophys. J. Int. (2018) **215,** 1474–1482
Advance Access publication 2018 August 24
GJI Gravity, geodesy and tides

doi: 10.1093/gji/ggy353

The use of object-oriented and process-oriented methods for gravity anomaly modelling of sedimentary basins

A.B. Watts

Department of Earth Sciences, University of Oxford, South Parks Road, Oxford OX1 3AN, *UK. E-mail: tony.watts@earth.ox.ac.uk*

Accepted 2018 August 22. Received 2018 August 20; in original form 2018 June 12

SUMMARY

Gravity anomalies have provided some of the most commonly accepted models we have for the density structure, stress state and strength of Earth's crust and lithosphere. Two approaches in the indirect approach to gravity interpretation have been followed. In one, Object-Oriented Gravity Modelling (OOGM), physical models are constructed for the geometry and density of a causative body and a 'trial and error' method is used to adjust the shape of a body until a satisfactory fit with observations is obtained. In another, Process-Oriented Gravity Modelling (POGM), one or more geological processes, such as sediment loading are considered, along with the density, and parameters such as the flexural rigidity of the lithosphere are varied until a fit is obtained. Both OOGM and POGM are based on the density structure and so should yield the same results. Curiously though, the two approaches have not yet been compared. We show here that in the case of a rifted continental margin that is subsequently loaded by sediment, OOGM and POGM do, in fact, yield the same gravity anomaly. Therefore, gravity anomalies yield information not only on the physical structure but also on geological processes in the past. We attribute this to the presence of an elastic 'core' that, irrespective of yielding, imparts on the lithosphere a 'memory' and allows gravity measurements made today to be used to infer past geological events.

Key words: Gravity anomalies and Earth structure; Sedimentary basin processes; Lithospheric flexure.

INTRODUCTION

It is traditional when modelling gravity anomalies to interpret them in terms of static density distributions in Earth's crust and upper mantle. Many of our most commonly accepted models for the structure of the crust and upper mantle, for example, at mid-ocean ridges (Talwani *et al.* 1965), passive (Worzel 1968) and active (Talwani *et al.* 1961) continental margins, have come from assuming the geometry and density of a causative body, calculating the gravity anomaly and comparing it to observations. Body parameters are then adjusted by a 'trial and error' method until a satisfactory fit between observed and calculated gravity anomalies has been obtained.

This approach, which we dub here Object-Oriented Gravity Modelling (OOGM), is useful as it constrains both the physical properties and geometry of a particular geological feature that causes an observed gravity anomaly. OOGM is, of course, fundamentally non-unique and there may be more than one set of body parameters that will explain a given gravity anomaly, as has been demonstrated by Skeels (1947), among others. Nevertheless, OOGM is a widely used approach, for example, to discriminate between subsurface granites and sedimentary basins (e.g. Bott 1988), mafic and ultramafic intrusions (e.g. Emeleus *et al.* 1997) and salt bearing and non-salt bearing anticlines (e.g. Edgell 1992). However, by itself OOGM provides little information about the processes that have been involved in the formation of a geological feature.

The first steps to a process-oriented rather than an object-oriented approach to gravity anomaly interpretation were taken by Gunn (1944) and Walcott (1972) who considered the gravity anomaly that would be expected at a margin of a continent or ocean. Gunn (1944) calculated the deformation expected from the emplacement of a sediment load on a tilted, differentially cooling, margin and the so-called gravity 'defect' that resulted from the combined effect of the load and deformation. His calculations revealed a high (up to +140 mGal) over the sediment load and a flanking, asymmetric low that reached its maximum amplitude (up to −70 mGal) on the *landward* side of the load which he compared it to an observed profile of the East Coast, US margin. While Gunn (1944) considered the initial margin as in isostatic equilibrium, he did not compute its gravity anomaly. Walcott (1972), in contrast, computed both the gravity anomaly associated with the initial margin and the sediment load and its isostatic compensation. His calculations revealed a high over the sediment load (up to +70 mGal) and a flanking, asymmetric low that reached its maximum amplitude (up to −70 mGal) on the *seaward* side of the load, which he then compared, in a general way, to observations over the Mississippi River Delta region. The difference in the asymmetry of the flanking lows between Gunn

(1944) and Walcott (1972) suggests that Walcott added the gravity anomaly of the initial margin to the gravity anomaly due to the sediment load and its flexural compensation before comparing the sum to observations, although he did not explicitly say that this was the case in his paper.

In 1988, Watts (1988) outlined a process-driven approach to gravity interpretation, dubbed later by Watts & Fairhead (1999) as Process-Oriented Gravity Modelling (POGM). In this approach, gravity anomalies are interpreted in terms of the processes believed to be responsible for the formation of a feature and the crustal (and mantle) structure is built through geological time. Simple isostatically balanced models for geological processes such as rifting (and associated crustal thinning), sedimentation, magmatism and erosion are constructed and the gravity anomalies calculated, summed and compared to observed gravity anomaly data. POGM does not eliminate the ambiguity in gravity interpretation, although it could be argued that it helps reduce it.

The first application of POGM was to shipboard gravity anomaly data over the Baltimore Canyon Trough in the East Coast, USA rifted margin where it was used to predict the crustal structure, isostatic parameters (e.g. the effective elastic thickness) and the most likely location of the ocean/continent boundary. Subsequent studies have applied POGM to sedimentary basins in other rifted margins notably those offshore New Zealand (Holt & Stern 1991), UK (Watts & Fairhead 1997), Gabon (Watts & Stewart 1998), Namibia (Stewart *et al.* 2000), India (Krishna *et al.* 2000), Mozambique (Watts 2001), Antarctica (Karner *et al.* 2005; Close *et al.* 2009), Brazil (Watts *et al.* 2009) and Argentina (Pedraza De Marchi *et al.* 2017), as well as to basins in strike-slip (Madon & Watts 1998) and certain cratonic (Haddad *et al.* 2001, Tozer *et al.* 2017) settings.

The OOGM and POGM approaches to gravity interpretation differ fundamentally in the way an observed gravity anomaly is modelled. OOGM considers only the physical structure of a causative body, in contrast to POGM, which considers the geological processes that form it. Both approaches are based, however, on the density structure and so should, in principle, yield the same results. Curiously, none of the studies cited above have quantitatively compared the two approaches.

The purpose of this paper is to compare the OOGM and POGM approaches to the indirect interpretation of gravity anomaly data. We find that OOGM and POGM do, in fact, yield the same results. Therefore, gravity anomalies measured today reflect not only the static density structure of Earth's crust and mantle but also processes that have occurred in the past and are now represented in the ancient rock record. We focus here on gravity anomalies over sedimentary basins, and apply OOGM and POGM to a sedimentary basin that developed in a rifted continental margin. We then compare the OOGM and POGM methodologies, offering reasons why they agree and suggestions as to which other geological processes POGM might be applied to in the future.

GRAVITY ANOMALIES OVER SEDIMENTARY BASINS

Sedimentary basins are infilled by material that has been derived, for example, by weathering of adjacent terrestrial source areas and carbonate production within the water column. Depending on the relative proportion of terrestrial and marine sediments and the degree of mechanical and chemical compaction, basins are usually lower in average density than surrounding crystalline basement rocks, sometimes by as much as 200–600 kg m^{-3}. The general observation that sedimentary basins are associated with negative gravity anomalies supports the suggestion that they are mass deficiencies. Notable examples include the strike-slip basins of the Dead Sea (Ten Brink *et al.* 1993), Opheus (Loncarevic & Ewing 1963), Vienna (Salcher *et al.* 2012) and the extensional basins of the Gulf of St. Lawrence (Langdon & Hall 1994), Celtic Sea (Sibuet *et al.* 1990), Irish Sea (Bott 1964) and Hebridean-Shetland shelf (Bott & Watts 1970).

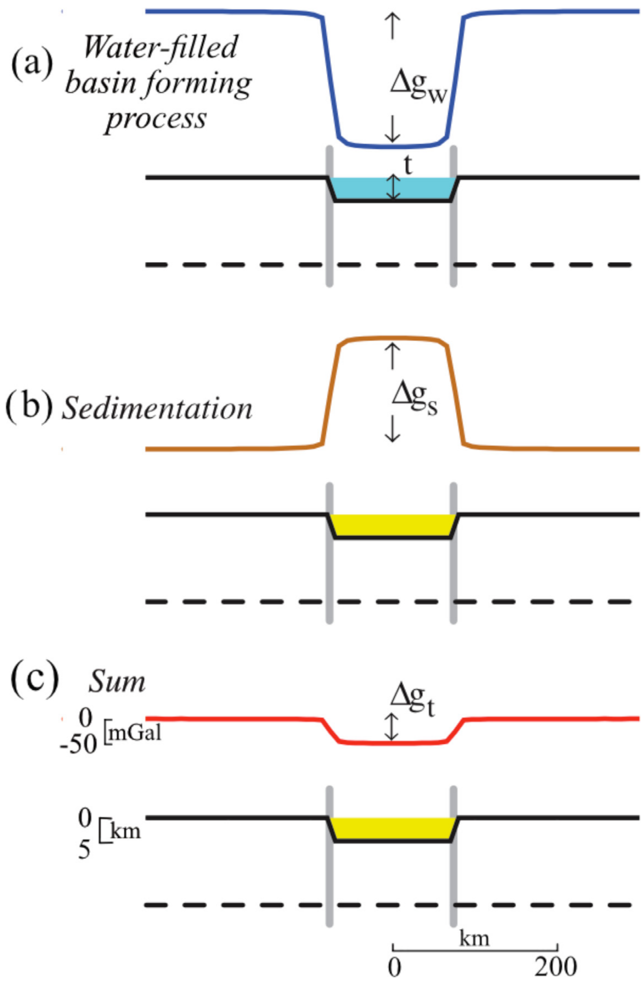

Figure 1. The gravity anomaly associated with a 100 km wide, 4 km deep, uncompensated, water-filled depression that is subsequently infilled by sediment. Vertical grey bars delineate the basin edge. (a) Gravity effect of the water-filled basin, assuming a density of water and crust of 1030 and 2800 kg m^{-3}, respectively. (b) Gravity effect of the sediment fill, assuming a density of sediment of 2400 kg m^{-3}. (c) Sum anomaly obtained by adding the gravity effects in (a) and (b). The dashed line represents a crustal interface beneath the basin. It is assumed here, there is no contribution to the gravity effect from this or any other interface beneath the basin, including the Moho.

The presence of a negative anomaly over a basin should not, however, be expected. Sediments are denser than the material they displace (air or water) and so will correlate with a positive, not a negative, gravity anomaly. This is the case, irrespective of whether or not the infilling sediments formed in a terrestrial or marine environment.

This paradox can be solved if we take a POGM, rather than an OOGM, approach to gravity interpretation. Consider, for example, the simple case of a 2-D uncompensated water-filled depression (i.e. a depression that extends infinitely in the along-axis $\pm y$ direction) that is subsequently filled to the 'brim' by sediment (Fig. 1). The

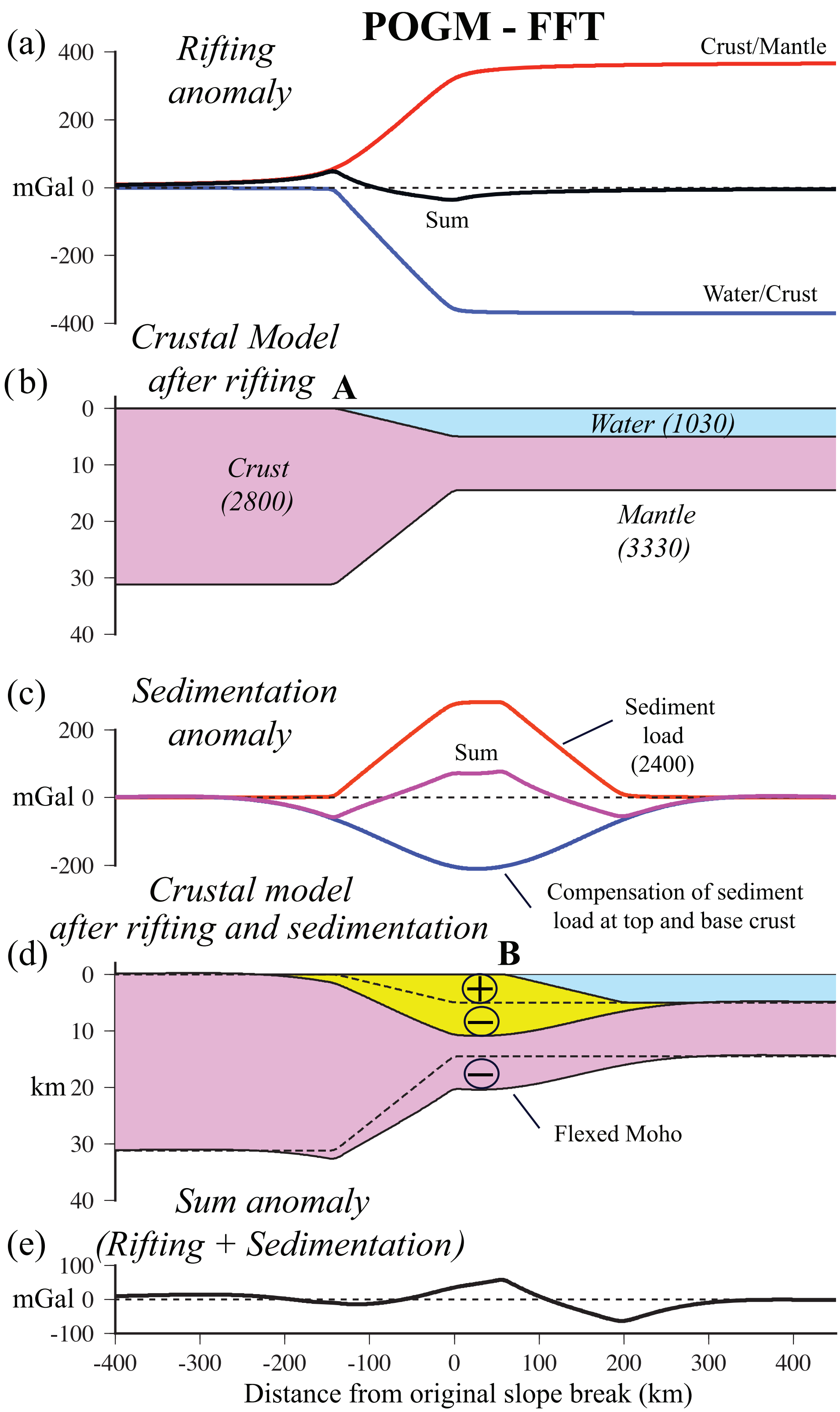

Figure 2. Process-Oriented Gravity Modelling (POGM) at a well-sedimented rifted continental margin. (a) The rifting gravity anomaly obtained by adding the gravity effect of the water-filled basin to the gravity effect of the elevated Moho. (b) Crustal model after rifting. (c) The sedimentation gravity anomaly obtained by adding the gravity effect of the sediment load (indicated by the bold circled + in panel d) and the gravity effect of its compensation at the top and base of the crust (indicated by the bold circled − in panel d). (d) Crustal model after rifting and sedimentation. Dashed lines show the original configuration of the margin. Solid lines with colour shading show the final configuration of the margin after sediment loading and flexure. (e) Sum gravity anomaly obtained by adding the rifting and sedimentation gravity anomaly. The parameters assumed in the calculations are given in Table 1.

principle term in the gravity anomaly, Δg_w, associated with the water-filled depression is given by

$$\Delta g_w = 2\pi G(\rho_w - \rho_c)t,$$

where G = universal gravitational constant, ρ_w and ρ_c are the densities of water and crust, respectively and t is the depth of the depression. Since $\rho_c > \rho_w$ the gravity anomaly is negative. Sediments then infill the depression, displacing the water. The main term in the gravity anomaly associated with the sediment, Δg_s, is given by

$$\Delta g_s = 2\pi G(\rho_s - \rho_w)t,$$

where ρ_s is the density of the sediment. Since $\rho_s > \rho_w$ the gravity anomaly is positive.

If the formation of the water-filled depression and the accumulation of sediment are the only geological processes that have been operative then the main term in the sum gravity anomaly, Δg_t, is given by

$$\Delta g_t = \Delta g_w + \Delta g_s = 2\pi G(\rho_s - \rho_c)t,$$

which is the same sign and magnitude as what would have been calculated if an OOGM rather than POGM approach had been followed. Thus, OOGM and POGM give the same sum gravity anomaly. This is despite the fact that in POGM we consider the sediments as a mass excess that contributes a positive, not a negative, gravity anomaly.

While the sum anomaly in Fig. 1(c) of ∼−20 to 40 mGal generally accounts for the magnitude of the anomaly observed in many strike-slip and some rift basins, it is significantly less than observed in foreland basins, such as Alberta, Allegheny (Committee on the Gravity Anomaly map of North America 1987), Llanos (Watts *et al.* 1995) and Himalaya (Lyon-Caen & Molnar 1983) where gravity anomalies form linear belts in excess of −200 to −300 mGal. We attribute these anomalies to differences in the crustal structure, with the narrower strike-slip basins showing little or no involvement of the Moho, in contrast to the wider foreland basins where Moho maybe significantly deeper than surrounding regions because of migrating thrust/fold loads in the orogenic belt that cause a flanking downward-crustal flexure, the amplitude of which depends on the flexural rigidity of the underlying crust and lithosphere.

Many sedimentary basins are associated with positive, not negative, gravity anomalies. Central gravity anomaly highs of up to +20–40 mGal, for example, characterize the Parentis (Pinet *et al.* 1987), North Sea (Central graben) (Ziegler 1977) and Sirte (Gumati & Kanes 1985) rifted basins, among others. The highs are attributed to a Moho that has been elevated locally due to crustal stretching, the gravity effect of which combines to reduce the amplitude of the negative anomaly associated with a water-filled depression and enhance the amplitude of the positive anomaly associated with the sediments. An elevated Moho is consistent with the seismic and tectonic subsidence and uplift data over these basins (e.g. North Sea). Other basins, with central gravity highs (best seen after subtraction of the negative gravity anomaly effect of the sediments), include the Michigan, Parnaíba and Congo cratonic basins (Watts *et al.* 2018). However, there is no seismic evidence for an elevated Moho beneath these basins and so the highs here have been attributed to dense mafic bodies in the lower continental crust and/or upper mantle.

Table 1. Summary of parameters assumed in Figs 1–4.

Parameter	Symbol	Value
Initial crustal thickness	T_c	31.2 km
Density of crust	ρ_c	2800 kg m^{-3}
Density of mantle	ρ_m	3330 kg m^{-3}
Density of sea water	ρ_w	1030 kg m^{-3}
Density of sediment	ρ_s	2400 kg m^{-3}
Density of infill	ρ_{infill}	2400 kg m^{-3}
Elastic thickness	T_e	25 km
Young's modulus	E	10^{12} Pa
Poisson's ratio	σ	0.25

RESULTS

The calculations in Fig. 1 are useful as they provide a physical basis for understanding gravity anomalies associated with sedimentary basins. But, they assume a water-filled depression and a sediment accumulation that are uncompensated. They therefore ignore isostasy and so the question remains as to whether a POGM or OOGM approach would yield the same results in the more general case that a state of isostasy prevails during rifting and sedimentation.

Fig. 2 shows an application of POGM to a sedimentary basin that develops in a continental margin setting by rifting, crustal thinning, sediment loading and associated flexure. We assume a mode of extension with a 'depth of necking' (Kooi *et al.* 1992) of 7.2 km, which corresponds with the parameters in Table 1 to Airy-type isostasy. Sediments are then assumed to prograde across the surface of the thinned crust such that the original shelf edge migrates seawards from a point A to a point B (Figs 2b and d), a horizontal distance of ∼150 km. We assume that the sediments act as a load on a pre-existing rifted margin which is flexed downwards immediately beneath the load and upwards in flanking regions, in a similar manner as would an elastic plate with a thickness, T_e, of 25 km overlying an inviscid fluid. T_e is determined by the flexural rigidity of the plate, D, which is a proxy for the long-term strength of the lithosphere, and is given by

$$D = \frac{E T_e^3}{12(1-\sigma^2)}$$

The gravity anomalies associated with the crustal structures in Figs 2(b) and (d) have been computed using a Fast Fourier Transform (FFT) method for calculating the gravity effect of an undulating interface of uniform density contrast (Parker 1972) and are shown complete to $n = 4$ terms in Parker's series expansion. The rifting anomaly (Fig. 2a) was computed from the sum of the gravity effect of the original shelf, slope/rise and adjacent abyssal plain and the gravity effect of its compensating elevated mantle 'antiroot'. The anomaly (Fig. 2a) shows the typical 'edge-effect' high and flanking low associated with the transition from thick to thin crust. The sedimentation anomaly (Fig. 2c) was computed from the sum of the gravity effect of the sediment load (defined as the region between the initial and final shelf, slope/rise and adjacent abyssal plain) and the gravity effect of the compensating top and base of the crust. Importantly, we considered the sediment load and its compensating masses as three separate bodies with density contrasts with their surroundings of +1370 (where sediment displaces water), −400 (where sediment replaces crust) and −530 (where crust replaces mantle) kg m^{-3}, respectively, not as single interfaces. The gravity effect of each body is calculated by applying the FFT to *both* the upper and lower interfaces of each body. The sedimentation anomaly (Fig. 2c) shows a broad high flanked by lows, the peak of which is located over the

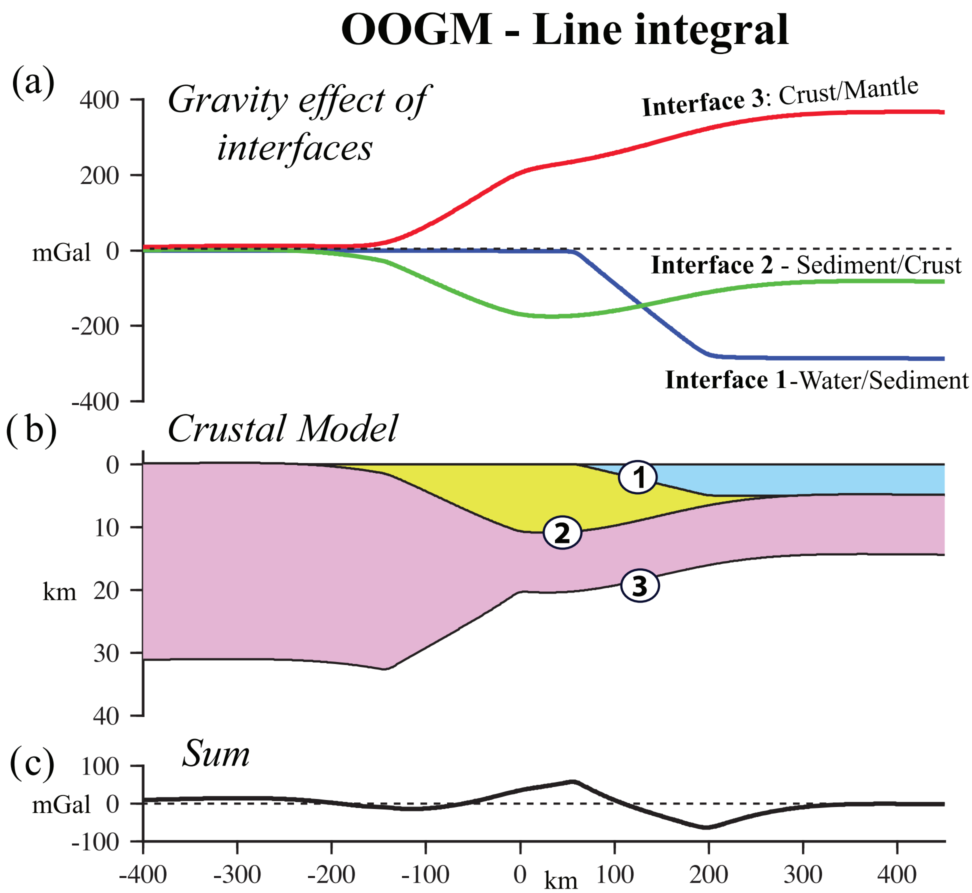

Figure 3. Object-Oriented Gravity Modelling (OOGM) at a well-sedimented rifted continental margin. (a) The gravity effect of the three interfaces (water/sediment—blue solid line, sediment/crust—green solid line and crust/mantle—red solid line) that make up the crustal model in Fig. 2(d). The gravity anomaly was computed using the density contrast across each interface and the line-integral method of Talwani *et al.* (1959) and Bott (1960). Interfaces have been extended horizontally to ±5000 km in order to avoid edge effects. (b) Crustal model showing the three interfaces. (c) Sum anomaly obtained by adding the gravity effect of the three interfaces.

thickest sediment. The sum anomaly (Fig. 2e), which was calculated by adding the rifting and sedimentation anomalies, reflects the gravity anomaly assuming the continental margin formed only by rifting and sedimentation and shows an ‘edge-effect’ anomaly high, similar in form to the rifting anomaly, but displaced seawards such that the high is located over the new position of the shelf edge. The high is flanked by two lows, one of smaller amplitude over the inner shelf and the other of larger amplitude over the abyssal plain, which together reflect the compensation of the sediment load.

In order to evaluate whether POGM and OOGM would give similar results, we then took the POGM crustal structure in Fig. 2(d) and calculated the sum gravity anomaly using an OOGM approach. To accomplish this, the crustal structure was divided into three interfaces at the water/sediment, sediment/crust and crust/mantle boundaries and the gravity effects calculated using the 2-D line integral methods of Talwani *et al.* (1959) and Bott (1960). We assumed a structure that is closed in a −x direction and open in a +x direction, and uniform density contrasts across the three interfaces of −1370 (where water is in contact with sediment), −400 (where sediment is in contact with crust) and −530 (where crust is in contact with mantle) kg m^{-3}, respectively.

It is noted here that OOGM is a fundamentally different way to model an observed gravity anomaly than POGM. Unlike POGM, OOGM takes no account of geological processes and so ignores the original and final position of the shelf break and the distribution of the sediment load and its isostatic compensation. Nevertheless, the sum anomaly of the three interfaces obtained by OOGM (Fig. 3c) closely resembles the sum anomaly obtained by POGM (Fig. 2e) with its characteristic ‘edge-effect’ high and flanking lows.

Fig. 4 shows a detailed comparison of the sum anomalies derived using POGM and OOGM. The mean difference between the sum anomaly in OOGM based on the three interfaces and the line integral method (Fig. 3) and POGM based on crustal thinning and sediment loading (Fig. 2) is −0.31 mGal and the standard deviation is 1.13 mGal. These differences are small when compared to the peak-to-trough amplitude of the ‘edge-effect’ high and low which reaches ±60 mGal. The main differences occur over the relatively steep slopes of the original and final shelf slope/rise and are attributed to artefacts in the FFT methodology, which uses Green’s Equivalent Theorem to replace a gravity anomaly by a surface mass at the mean depth of an interface. To verify this, we used OOGM with the same bodies as were used in the FFT calculation and compared it instead to the OOGM based on three interfaces. The mean difference between the two OOGM sum anomalies is 0.55 mGal and the standard deviation is 0.03 mGal. These comparisons suggest that irrespective of the methods used in OOGM (whether FFT or line integral—interface or body) the differences between POGM and OOGM are small and less than 1 per cent of the peak-to-trough sum anomaly.

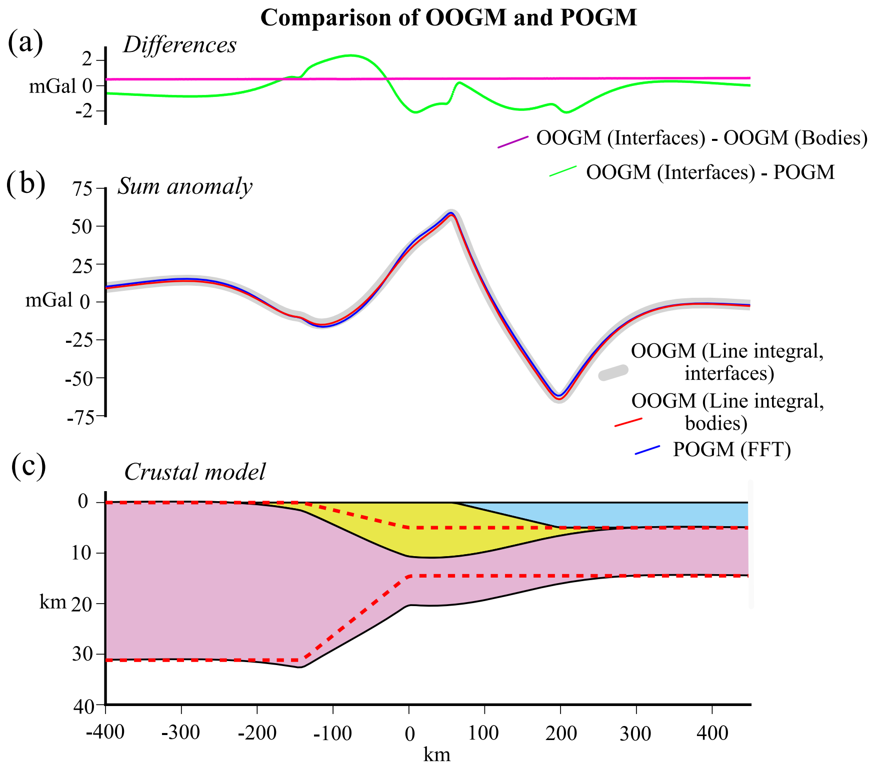

Figure 4. Comparison of POGM and OOGM techniques at a well-sedimented rifted margin. (a) The difference between OOGM and POGM sum anomalies, (b) sum anomalies computed using OOGM with line-integral interfaces and bodies and POGM and (c) crustal model. The red dashed lines show the original configuration of the margin, prior to sediment loading and flexure.

As stated previously, the interfaces used here in OOGM were derived from the POGM crustal structure. Both crustal models are based on isostasy and so it could be argued that the similarity between the OOGM and POGM sum anomalies shown in Fig. 4 is not surprising. However, the OOGM approach takes no account of process, in contrast to the POGM approach, which explicitly defines the mode of extension during rifting and the geometry of the sediment load and its isostatic compensation. We have shown in Fig. 4 that if the sediment thickness and underlying Moho are well enough constrained, say from seismic data, then an interpreter using the OOGM and POGM approaches will derive a similar sum gravity anomaly. If, on the other hand, the Moho cannot be seismically defined and only the sediment thickness is known, then an OOGM interpreter might, in the absence of deep crustal information, calculate the gravity anomaly assuming the sediments, and perhaps even the water, are uncompensated. Irrespective, the difference between OOGM and POGM would be stark, as Fig. 5 shows. In the case that the sediments are uncompensated and the water is compensated (e.g. by crustal thinning) OOGM yields a sum gravity anomaly high of a few hundred mGal, in contrast to POGM which yields a high of only a few tens of mGal. The figure illustrates the overall advantage of POGM over OOGM: POGM provides the interpreter with a sum gravity anomaly which is similar in amplitude and wavelength to the ubiquitous free-air 'edge-effect' gravity anomaly at rifted margins and a plausible model of the crustal structure based on geological processes whereas OOGM, which ignores process, provides a sum anomaly which is significantly larger in amplitude and longer in wavelength than observations and might (incorrectly) be interpreted in terms of localized changes in crustal thickness and/or lateral changes in density in the lower crust or upper mantle.

DISCUSSION

The demonstration in Fig. 4 that OOGM and POGM produce essentially the same sum anomalies is significant. While the demonstration has been conducted using models rather than observations, it confirms that gravity anomalies reflect not only the static density structure of a subsurface body but also the geological processes responsible for its formation.

The reasons for this can be sought in our understanding of how Earth responds to load shifts on its surface and in the nature of the isostatic mechanism. We know from flexure studies, for example, that the thickness of the lithosphere that supports a load is initially thick and of the order of the seismic thickness (e.g. Watts *et al.* 2013). As time elapses, the lithosphere relaxes and stresses migrate upwards from its low-viscosity hotter lower layers to its high-viscosity colder (essentially elastic) upper layers. The thickness of this layer determines the strength of the lithosphere, which, depending on load size, is limited by brittle failure in its uppermost part and ductile deformation in its lower part. The elastic 'core' (Watts & Burov 2003) that remains following yielding gives the lithosphere a 'memory' such that the flexure, together with its associated gravity anomalies, are in effect 'frozen in' and do not change significantly with time. Thus, the gravity anomaly measured today will reflect past geological events. It is the reason, for example, why the gravity anomaly can be used to determine the tectonic setting of bathymetric features in the geological past (Watts *et al.* 1980), why the gravity anomalies at extinct mid-ocean ridges resemble so closely those at active ridges (Watts 1982) and why the gravity anomaly 'edge effect' at Precambrian shield terrain boundaries (Gibb & Thomas 1976) are preserved for such long periods of time (>1 Ga).

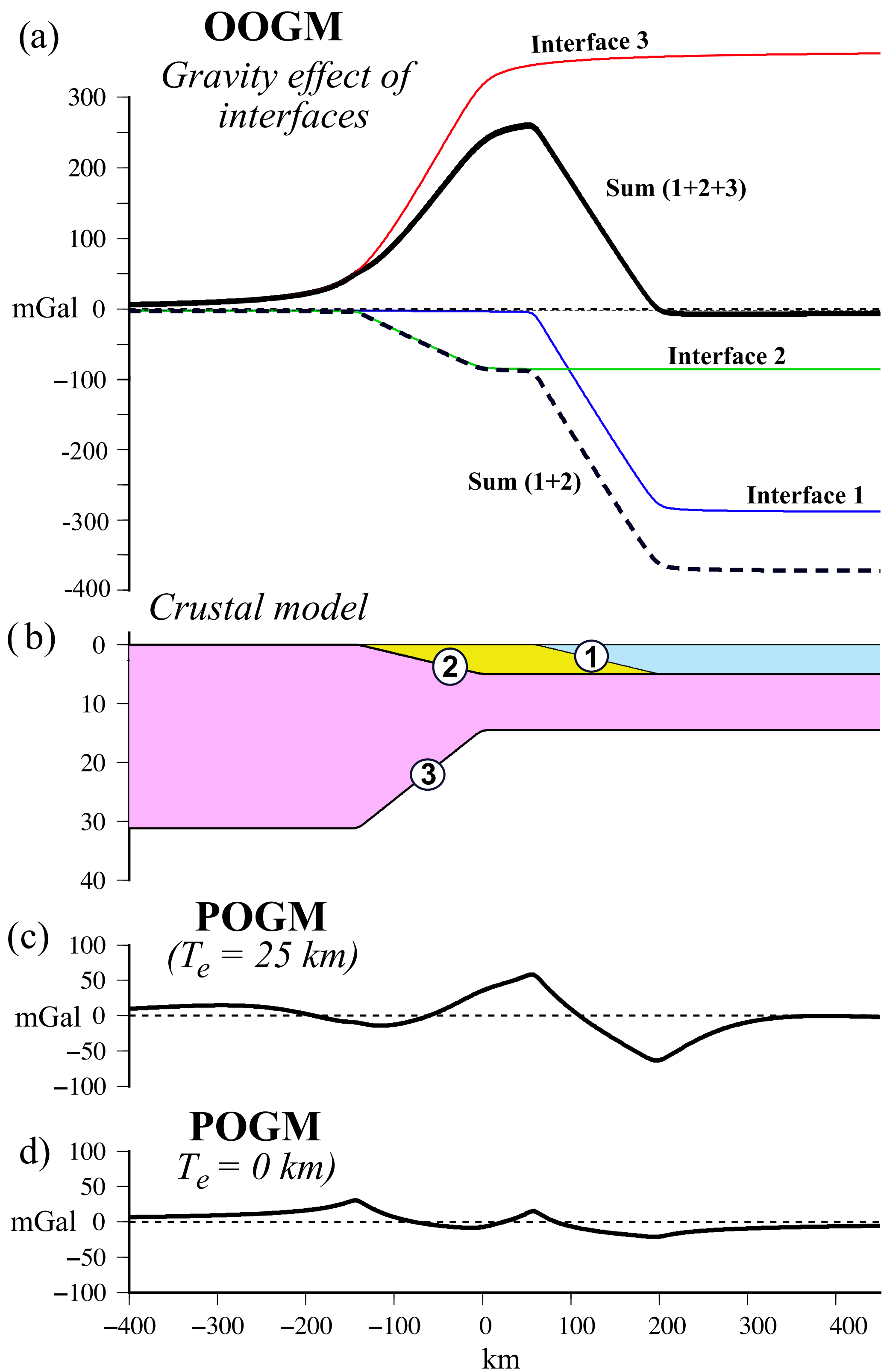

Figure 5. Comparison of the sum gravity anomaly expected for an OOGM approach assuming uncompensated sediment to a POGM approach in which the sediments are compensated. (a) The uncompensated sediment case. The gravity effect of the three interfaces (water/sediment—blue solid line, sediment/crust—green solid line and crust/mantle—red solid line) that make up the crustal model in (b) are shown. Gravity anomalies were computed using the same density contrasts across each interface as used in Fig. 3 and the line-integral method of Talwani *et al.* (1959) and Bott (1960). Interfaces have been extended horizontally to ±5000 km in order to avoid edge effects. Thick black lines show the sum gravity anomaly of the water and sediment (dashed) and water, sediment and crust (solid). (b) Crustal model showing the three interfaces. (c) POGM sum anomaly based on flexural compensation with T_e = 25 km. (d) POGM sum anomaly based on Airy-type compensation (i.e. T_e = 0 km). Note that in this case there are two highs: one over the initial and the other over the final shelf edge.

The long-term, essentially elastic, response of the lithosphere to loading confirms that POGM can be applied not only in a forward way, as carried out in this paper, but also in an inverse way. For example, the depth of water at the time of rifting can be derived by flexural backstripping of the sediment thickness derived from depth-migrated seismic reflection profile data, assuming different values of the elastic thickness, and used to predict the crustal structure and gravity anomaly associated with rifting. Sediments can then be loaded back onto the thinned crust and used to calculate the change in crustal structure and gravity anomaly that results from sedimentation. By comparing observations with the calculated sum gravity anomalies and the final crustal structure we can then determine whether simple models for rifting and sedimentation can explain the data or whether other geological processes have been involved. For example, the gravity anomaly maybe 'skewed' compared to the observed anomaly because of lateral variations in T_e and the seismically constrained Moho maybe shallower or deeper than calculated suggesting that material may have been added to the base of the crust since rifting by magmatic underplating or subtracted from the base by tectonic erosion.

Other, longer wavelength, departures in the gravity anomaly and the depth to Moho might arise from thermal isostasy. Depending on the age of a rifted margin, the juxtaposition of relatively cold-continental lithosphere against relatively hot-oceanic lithosphere could create temperature gradients and hence lateral density contrasts that extend further down than the base of the crust to the base of the thermal lithosphere and cause departures in both the gravity anomalies (Breivik *et al.* 1999) and the Moho depth (Chappell & Kusznir 2008), especially at relatively young rifted margins.

The models we have used in this paper are simple and only take into account rifting, uniform (Airy-type) crustal thinning and constant density sediment loading. POGM can easily be modified, however, to include non-uniform extension with depth (Royden & Keen 1980), strength during rifting (Watts & Stewart 1998) and a density distribution in the sediment that varies exponentially with depth (Granser 1987). Irrespective, the close agreement between the POGM and OOGM methodologies using simple models suggests that POGM might be a useful approach to adopt when modelling the gravity anomaly and crustal structure associated with other geological processes. These other processes include, but are not limited to, magmatic underplating, intracrustal thrusting, seaward-dipping reflector formation, granite emplacement and ophiolite obduction.

CONCLUSIONS

(1) POGM is a useful approach to adopt in gravity interpretation that provides information on the processes responsible for the formation of a particular geological feature.

(2) POGM is based on the density structure of loads and their isostatic compensation and yields the same results as OOGM.

(3) The similarity between POGM and OOGM is attributed to the lithosphere's elastic 'core' which gives it a 'memory' such that the flexures and gravity anomalies associated with past events are, in effect, 'frozen in' for long periods of time.

(4) The gravity anomalies measured today therefore, take on a special significance as they reflect past tectonic events. This appears to be the case despite the possibility that they might become involved in later deformation such as load age-dependent weakening, thermal age-dependent strengthening and structural inversion.

ACKNOWLEDGEMENTS

The author is grateful to the many former graduate students who through their involvement with POGM have helped shape some of the ideas expressed in this paper, especially Gary Karner, Jonathan Stewart, Paul Wyer, Catherine Allsop (née Marr), David Close and Brook Tozer. Ron Hackney (Geoscience Australia), Tim Stern (Victoria University, Wellington, New Zealand) and Rebecca Morgan (University of Oxford) are thanked for their insightful and helpful reviews of an early version of the manuscript. A MATLAB script to carry out the POGM calculations in Fig. 2 is available from the author.

REFERENCES

Bott, M.H.P., 1960. The use of rapid digital computing methods for direct gravity interpretation of sedimentary basins, *Geophys. J. R. astr. Soc.,* **3,** 63–67.

Bott, M.H.P., 1964. Gravity measurements in the north-eastern part of the Irish Sea, *Q. J. Geol. Soc.,* **120,** 369–394.

Bott, M.H.P., 1988. The Market Weighton gravity anomaly—granite or graben?, *Proc. Yorkshire Geol. Soc.,* **47,** 47–53.

Bott, M.H.P. & Watts, A.B., 1970. Deep sedimentary basins proved in the Hebridean-Shetland continental shelf and margin, *Nature,* 225–265.

Breivik, A.J., Verhoef, J. & Faleide, J.I., 1999. Effect of thermal contrasts on gravity modeling at passive margins: results from the western Barents Sea, *J. geophys. Res.,* **104,** 15 293–15 311.

Chappell, A.R. & Kusznir, N.J., 2008. Three-dimensional gravity inversion for Moho depth at rifted continental margins incorporating a lithosphere thermal gravity anomaly correction, *Geophys. J. Int.,* **174,** 1–13.

Close, D.I., Watts, A.B. & Stagg, H.M.J., 2009. A marine geophysical study of the Wilkes Land rifted continental margin, Antarctica, *Geophys. J. Int.,* **177,** 430–450.

Committee for the gravity anomaly map of North America, 1987. Continental-Scale Map 002, Scale 1:5 000 000, 5 sheets, Geological Society of America.

Edgell, H.S., 1992. Basement tectonics of Saudi Arabia as related to oil field structures, in *Basement Tectonics 9,* pp. 169–193, eds Rickard, M.J. , Williams, P.R. *et al.*, Kluwer Academic Publishers.

Emeleus, C.H., Gallagher, M.J. & Peacock, J.D., 1997. *Geology of Rum and the Adjacent Islands: Memoir for 1:50 000 Geological Sheet 60 (Scotland),* The Stationery Office for British Geological Survey.

Gibb, R.A. & Thomas, M.D., 1976. Gravity signature of fossil plate boundaries in the Canadian Shield, *Nature,* **262,** 199–200.

Granser, H., 1987. Three-dimensional interpretation of gravity data from sedimentary basins using an exponential density-depth function, *Geophys. Prospect.,* **35,** 1030–1041.

Gumati, Y.D. & Kanes, W.H., 1985. Early tertiary subsidence and sedimentary facies–northern Sirte basin, Libya, *Am. Assoc. Petrol. Geol. Bull.,* **69,** 39–52.

Gunn, R., 1944. A quantitative study of the lithosphere and gravity anomalies along the Atlantic coast, *J. Franklin Inst.,* **237,** 139–154.

Haddad, D., Watts, A.B. & Lindsay, J., 2001. Evolution of the intracratonic Officer Basin, central Australia: implications from subsidence analysis and gravity modelling, *Basin Res.,* **13,** 217–238.

Holt, W.E. & Stern, T.A., 1991. Sediment loading on the western platform of the New Zealand continent : implications for the strength of a continental margin, *Earth planet. Sci. Lett.,* **107,** 523–538.

Karner, G.D., Studinger, M. & Bell, R.E., 2005. Gravity anomalies of sedimentary basins and their mechanical implications: application to the Ross Sea basins, West Antarctica, *Earth planet. Sci. Lett.,* **235,** 577–596.

Kooi, H., Cloetingh, S. & Burrus, J., 1992. Lithospheric necking and regional isostasy at extensional basins: 1. Subsidence and gravity modeling with an application to the Gulf of Lions Margin (SE France), *J. geophys. Res.,* **97**(B12), 17 553–17 571.

Krishna, M.R., Chand, S. & Subrahmanyam, C., 2000. Gravity anomalies, sediment loading and lithospheric flexure associated with the Krishna-Godavari basin, eastern continental margin of India, *Earth planet. Sci. Lett.,* **175,** 223–232.

Langdon, G.S. & Hall, J., 1994. Devonian-Carboniferous tectonics and basin deformation in the Cabot Strait area, eastern Canada, *Am. Assoc. Petrol. Geol. Bull. ,* **78,** 1748–1774.

Loncarevic, B.D. & Ewing, G.N., 1963. Geophysical study of the Orpheus gravity anomaly, in *The Proceedings of the Seventh World Petroleum Congress,* pp. 827–835, Mexico City, MX.

Lyon-Caen, H. & Molnar, P., 1983. Constraints on the structure of the Himalaya from an analysis of gravity anomalies and a flexural model of the lithosphere, *J. geophys. Res.,* **88,** 8171–8191.

Madon, M.B. & Watts, A.B., 1998. Gravity anomalies, subsidence history and the tectonic evolution of the Malay and Penyu Basins (offshore Peninsular Malaysia), *Basin Res.,* **10,** 375–392.

Parker, R.L., 1972. The rapid calculation of potential anomalies, *Geophys. J. R. astr. Soc.,* **31,** 447–455.

Pedraza De Marchi, A.C., Ghidella, M.E. & Tocho, C.N., 2017. 3D Process-Oriented Gravity Modelling applied north of 49°S on the Argentine continental margin, *J. South Am. Earth Sci.,* **81,** 177–188.

Pinet, B. *et al.*, 1987. Crustal thinning on the Aquitaine shelf, Bay of Biscay, from deep seismic data, *Nature,* **325,** 513–516.

Royden, L. & Keen, C.E., 1980. Rifting process and thermal evolution of the continental margin of Eastern Canada determined from subsidence curves, *Earth planet. Sci. Lett.,* **51,** 343–361.

Salcher, B.C., Meurers, B., Smit, J., Decker, K., Hölzel, M. & Wagreich, M., 2012. Strike-slip tectonics and Quaternary basin formation along the Vienna Basin fault system inferred from Bouguer gravity derivatives, *Tectonics,* **31**(3).

Sibuet, J.C., Dyment, J., Bois, C., Pinet, B. & Ondreas, H., 1990. Constraints on the formation of Celtic sea basins from gravity data and deep seismic profiles, in *The Potential of Deep Seismic Profiling for Hydrocarbon Exploration,* pp. 355–379, eds Pinet, B. & Bois, C., Éditions Technip.

Skeels, D.C., 1947. Ambiguity in gravity interpretation, *Geophysics,* **12,** 43–56.

Stewart, J., Watts, A.B. & Bagguley, J., 2000. Three-dimensional subsidence analysis and gravity modelling of the continental margin offshore Namibia, *Geophys. J. Int.,* **141,** 724–746.

Talwani, M., Worzel, J.L. & Landisman, M., 1959. Rapid gravity computations for two-dimensional bodies with application to the Mendocino submarine fracture zone, *J. geophys. Res.,* **64,** 49–59.

Talwani, M., Worzel, J.L. & Ewing, M., 1961. Gravity anomalies and crustal section across the Torga Trench, *J. geophys. Res.,* **66,** 1265–1278.

Talwani, M., LePichon, X. & Ewing, M., 1965. Crustal structure of the mid-ocean ridges: 2. Computed model from gravity and seismic refraction data, *J. geophys. Res.,* **70,** 341–352.

Ten Brink, U.S., Ben Avraham, Z., Bell, R.E., Hassouneh, M., Coleman, D.F., Andreasen, G., Tibor, G. & Coakley, B., 1993. Structure of the Dead Sea pull-apart basin from gravity analysis, *J. geophys. Res.,* **98,** 21 887–21 894.

Tozer, B., Watts, A.B. & Daly, M.C., 2017. Crustal structure, gravity anomalies and subsidence history of the Parnaíba cratonic basin, Northeast Brazil, *J. geophys. Res.,* **122,** 5591–5621.

Walcott, R.I., 1972. Gravity, flexure, and the growth of sedimentary basins at a continental edge, *Bull. geol. Soc. Am.,* **83,** 1845–1848.

Watts, A.B., 1982. Gravity anomalies over oceanic rifts, in *Continental and Oceanic Rifts,* pp. 99–106, ed. Pálmason, G., American Geophysical Union.

Watts, A.B., 1988. Gravity anomalies, crustal structure and flexure of the lithosphere at the Baltimore Canyon Trough, *Earth planet. Sci. Lett.,* **89,** 221–238.

Watts, A.B., 2001. Gravity anomalies, flexure and crustal structure at the Mozambique rifted margin, *Mar. Pet. Geol.,* **18,** 445–455.

Watts, A.B. & Burov, E.B., 2003. Lithospheric strength and its relationship to the elastic and seismogenic layer thickness, *Earth planet. Sci. Lett.,* **213,** 113–131.

Watts, A.B. & Fairhead, J.D., 1997. Gravity anomalies and magmatism at the British Isles continental margin, *J. geol. Soc. Lond.,* **154,** 523–529.

Watts, A.B. & Fairhead, J.D., 1999. A process oriented approach to modeling the gravity signature of continental margins, *Leading Edge,* **18,** 258–263.

Watts, A.B. & Stewart, J., 1998. Gravity anomalies and segmentation of the continental margin offshore West Africa, *Earth planet. Sci. Lett.,* **156,** 239–252.

Watts, A.B., Bodine, J.H. & Ribe, N.M., 1980. Observations of flexure and the geological evolution of the Pacific Ocean basin, *Nature,* **283,** 532–537.

Watts, A.B., Lamb, S.H., Fairhead, J.D. & Dewey, J.F., 1995. Lithospheric flexure and bending of the Central Andes, *Earth planet. Sci. Lett.,* **134,** 9–21.

Watts, A.B., Rodger, M., Peirce, C., Greenroyd, C.J. & Hobbs, R.W., 2009. Seismic structure, gravity anomalies, and flexure of the Amazon continental margin, NE Brazil, *J geophys. Res.,* **114**.

Watts, A.B., Zhong, S.J. & Hunter, J., 2013. The behavior of the lithosphere on seismic to geologic timescales, *Annu. Rev. Earth Planet. Sci.,* **41,** 443–468.

Watts, A.B., Tozer, B., Daly, M.C. & Smith, J., 2018. A comparative study of the Parnaíba, Michigan and Congo cratonic basins, in *Cratonic Basin Formation: A Case Study of the Parnaíba Basin of Brazil,* eds Daly, M.C., Fuck, R.A., Julia, J., Macdonald, D.I. & Watts, A.B., Geological Society of London.

Worzel, J.L., 1968. Advances in marine geophysical research of continental margins, *Can. J. Earth Sci.,* **5,** 963–983.

Ziegler, P.A., 1977. Geology and hydrocarbon provinces of the North Sea, *GeoJournal,* **1**(1), 7–32.